Effect of surfactant on the stability of film flow down an inclined plane

By M. G. BLYTH[1] AND C. POZRIKIDIS[2]

[1]School of Mathematics, University of East Anglia, Norwich, NR4 7TJ, UK

[2]Department of Mechanical and Aerospace Engineering, University of California, San Diego, La Jolla, CA 92093-0411, USA

The effect of an insoluble surfactant on the stability of the gravity-driven flow of a liquid film down an inclined plane is investigated by a normal-mode analysis. Numerical solutions of the Orr–Sommerfeld equation reveal the occurrence of a stable Marangoni mode and a possibly unstable Yih mode, and demonstrate that the primary role of the surfactant is effectively to raise the critical Reynolds number at which instability is first encountered.

1. Introduction

It has long been recognized that an insoluble surfactant has a stabilizing influence on the gravity-driven flow of a liquid film down an inclined or vertical wall, by raising the critical Reynolds number above which the basic Nusselt unidirectional flow becomes susceptible to infinitesimal perturbations (Benjamin 1964; Whitaker 1964). Supporting theoretical evidence has been provided by several authors based on a linear stability analysis of the Nusselt unidirectional flow, properly generalized to accommodate the Marangoni traction due to surfactant surface concentration variations. Motivation for these studies has been provided by the pervasiveness of film flows in various branches of modern and traditional technology, and more specifically, by the opportunity to control these flows by manipulating their surface properties by the use of surfactants. For example, in precision liquid coating encountered in the manufacturing of photographic films, stable film flows of solitary or superposed layers are of paramount importance in ensuring manufactured product quality, as reviewed by Weinstein & Ruschak (2004).

Whitaker (1964) presented numerical solutions of the Orr–Sommerfeld equation using approximate boundary conditions, and deduced a critical Reynolds number above which the film flow becomes unstable. In subsequent work, Whitaker & Jones (1966) and Lin (1970) developed a long-wave analysis, and derived an asymptotic prediction for the critical Reynolds number under this restricted framework. Anshus & Acrivos (1967) confirmed the critical Reynolds number for a vertically falling film, and showed that the surfactant significantly increases the wavelength of the most rapidly growing mode. In related work, Ji & Setterwall (1994) demonstrated the existence of an unstable Marangoni mode for vertical film flow in the presence of a soluble surfactant.

Pozrikidis (2003) recently carried out a linear stability analysis of the film flow in the presence of an insoluble surfactant in the limit of vanishing Reynolds number, and demonstrated the occurrence of two normal modes parameterized by the wavenumber. The first is essentially the classical Yih (1963) mode of the pure film flow, whereas the second is a Marangoni mode associated with the presence of the surfactant. Physically,
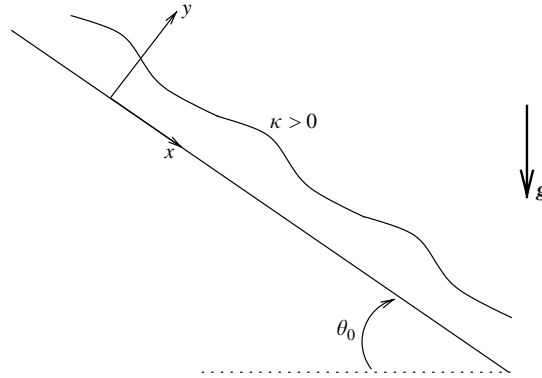
FIGURE 1. Schematic illustration of gravity-driven film flow down an plane wall that is inclined at an angle θ_0 with respect to the horizontal.

the Marangoni mode arises from the local variations in the surface tension generated by the surfactant. These variations induce local Marangoni flows which may either promote instability by feeding fluid into the troughs and crests of a perturbation wave, or else ameliorate a disturbance by draining fluid away from the troughs and crests. In fact, analytical solutions of the Orr–Sommerfeld equation for Stokes flow have revealed that an insoluble surfactant promotes the decay of the Yih mode. However, because the rate of decay of the Marangoni mode is lower than that of the Yih mode, the surfactant can be said to have a destabilizing influence.

These recent results on Stokes flow seem to contradict the earlier results on the critical Reynolds number for flow instability. To resolve this apparent inconsistency and demonstrate the precise effect of the surfactant, in this article we present numerical solutions of the linear stability problem at arbitrary Reynolds numbers. The results will show that the Marangoni mode remains stable under all conditions considered, the Yih mode dominates the instability at sufficiently high Reynolds numbers, and the surfactant has an overall stabilizing influence.

2. Formulation of the linear stability problem

We consider the gravity-driven flow of a liquid film down a plane wall that is inclined at an angle θ_0 to the horizontal, as shown in figure 1. The surface of the film is occupied by an insoluble surfactant with surface concentration Γ, which is convected and diffuses over the interface, but not into the bulk of the fluids, to locally alter the surface tension, γ. Since the perturbed film flow is assumed to be two-dimensional, it is convenient to introduce a streamfunction $\psi(x, y, t)$, defined so that that x and y velocity components are given by $u_x = \partial\psi/\partial y$, $u_y = -\partial\psi/\partial x$.

In the unperturbed configuration, the surface of the film is flat, and the unperturbed surfactant concentration is assumed to be uniform and equal to Γ_0, corresponding to the unperturbed surface tension γ_0. Accordingly, the shear stress is zero at the free surface, and the flow is described by the Nusselt solution with velocity, streamfunction, and free-surface velocity, U_s, given by given by

$$\left.\begin{aligned} u_x^{(0)} &= \frac{\rho g \sin\theta_0}{2\mu} y(2h - y), \qquad u_y^{(0)} = 0, \\ \psi^{(0)} &= \frac{\rho g \sin\theta_0}{2\mu} y^2\left(h - \tfrac{1}{3}y\right), \quad U_s = \frac{\rho g h^2 \sin\theta_0}{2\mu}, \end{aligned}\right\} \tag{2.1}$$

where g is the acceleration due to gravity, ρ is the liquid density, μ is the liquid viscosity, and h is the film thickness.

Our goal is to assess the linear stability of the film flow with respect to two-dimensional, spatially periodic perturbations of wavelength L. The perturbed flow is governed by the Navier–Stokes equation and the continuity equation for incompressible fluids, subject to the no-slip and no-penetration conditions at the wall. At the free surface, the traction f is required to satisfy the boundary condition

$$f \equiv \boldsymbol{\sigma} \cdot \boldsymbol{n} = -(\gamma \kappa + p_a)\boldsymbol{n} - \frac{\partial \gamma}{\partial l} \boldsymbol{t}, \qquad (2.2)$$

where $\boldsymbol{\sigma}$ is the Newtonian stress tensor, $\boldsymbol{n}$ is the unit normal vector pointing into the film, $\boldsymbol{t}$ is the unit tangent vector pointing in the direction of increasing arclength l, p_a is the atmospheric pressure, and κ is the interfacial curvature in the (x, y)-plane, reckoned to be positive when the surface is downward parabolic, as indicated in figure 1.

The surface surfactant concentration, $\Gamma(x, t)$, evolves according to the transport equation

$$\frac{\mathrm{d}\Gamma}{\mathrm{d}t} + u_t \frac{\partial \Gamma}{\partial l} + \Gamma \left(\frac{\partial u_t}{\partial l} + \kappa u_n \right) = D_s \frac{\partial^2 \Gamma}{\partial l^2}, \qquad (2.3)$$

where $u_t = \boldsymbol{u} \cdot \boldsymbol{t}$ and $u_n = \boldsymbol{u} \cdot \boldsymbol{n}$ are the interfacial velocities in the directions of the tangential and normal vector, respectively, and D_s is the surface surfactant diffusivity (e.g. Li & Pozrikidis 1997; Yon & Pozrikidis 1998). The derivative $\mathrm{d}/\mathrm{d}t$ on the left-hand side of (2.3) expresses the rate of change of a variable following the motion of interfacial nodes moving with the component of the fluid velocity normal to the interface. The second term on the left-hand side of (2.3) represents the effect of surface convection, while the terms enclosed by the parentheses represent the effect of surfactant dilatation due to in-plane stretching and expansion due to motion in the normal direction. In practice, the surfactant diffusivity D_s is typically small, and the effect of surfactant diffusion is of secondary consideration.

The fluid is subjected to spatially periodic perturbations that displace the otherwise flat surface to a position described by $y = h + \eta(x, t)$, where the magnitude of η is assumed to be small compared to the unperturbed film thickness, h. For a normal-mode perturbation with wavenumber $k = 2\pi/L$, the waveform of the surface disturbance is described as $\eta(x, t) = A_1 \exp(ik[x - ct])$, where A_1 is a complex amplitude, and $c = c_r + ic_i$ is the complex wave speed. The streamfunction, pressure, and surfactant concentration are written in the corresponding forms

$$\left.\begin{array}{l} \psi = \psi^{(0)}(y) + \psi^{(1)}(y)\mathrm{e}^{ik(x-ct)}, \quad p = p^{(0)}(y) + p^{(1)}(y)\mathrm{e}^{ik(x-ct)}, \\[6pt] \Gamma = \Gamma_0 + \Gamma_1 \mathrm{e}^{ik(x-ct)}. \end{array}\right\} \qquad (2.4)$$

Linearizing the kinematic condition at the interface, $\mathrm{D}[y - \eta(x, t)]/\mathrm{D}t = 0$, we find

$$\psi^{(1)}(y = h) = -U_s \zeta A_1, \qquad (2.5)$$

where $\mathrm{D}/\mathrm{D}t$ is the material derivative, and we have defined $\zeta \equiv 1 - c/U_s$. On eliminating the pressure from the linearized form of the normal component of the dynamic surface condition (2.2) using the x-component of the momentum equation, we obtain

$$\mu \frac{\mathrm{d}^3 \psi^{(1)}}{\mathrm{d}y^3} - k[3k\mu + i\rho U_s \zeta] \frac{\mathrm{d}\psi^{(1)}}{\mathrm{d}y} = ik[\rho g U_s \cos \theta_0 + \gamma_0 k^2] A_1, \qquad (2.6)$$

where all terms are evaluated at $y = h$. Linearizing now the transport equation (2.3) taking into account that the basic flow experiences zero stress at the free surface, we obtain

$$\Gamma_1 = -\frac{\Gamma_0}{U_s \zeta - ik D_s} \frac{d\psi^{(1)}}{dy}, \qquad (2.7)$$

where the derivative on the right-hand side is evaluated at $y = h$. Substituting this expression in the linearized tangential component of the dynamic surface condition (2.2), we find

$$\mu \left(\frac{d^2 \psi^{(1)}}{dy^2} + k^2 \psi^{(1)} + A_1 \frac{d^2 u_x^{(0)}}{dy^2} \right) = \frac{ik\gamma_0 Ma}{U_s \zeta - ik D_s} \frac{d\psi^{(1)}}{dy}, \qquad (2.8)$$

where all terms are evaluated at $y = h$. The Marangoni number on the right-hand side is defined as $Ma = E\Gamma_0 / \gamma_0$, where E is the surface elasticity defined from the linearized interface equation of state, $\gamma = \gamma_0 - E(\Gamma - \Gamma_0)$. Finally, to satisfy the no-slip and no-penetration conditions at the wall, we require

$$\psi^{(1)} = \frac{d\psi^{(1)}}{dy} = 0 \qquad (2.9)$$

at $y = 0$.

Substituting (2.4) in the Navier–Stokes equation and linearizing, we arrive at the standard Orr–Sommerfeld equation (e.g. Pozrikidis 1997),

$$\left(\frac{d^2}{dy^2} - k^2 \right)^2 \psi^{(1)} = \frac{ik\rho}{\mu} \left[(u_x^{(0)} - U_s[1 - \zeta]) \left(\frac{d^2}{dy^2} - k^2 \right) \psi^{(1)} - \psi^{(1)} \frac{d^2 u_x^{(0)}}{dy^2} \right], \qquad (2.10)$$

which is to be solved subject to conditions (2.5)–(2.9).

A straightforward dimensional analysis reveals that the complex phase velocity of the perturbation depends on the reduced wavenumber kh and the Marangoni number Ma, the Reynolds number, Re, the capillary number, Ca, and a dimensionless property group α, defined as

$$Re = \frac{\rho U_s h}{\mu}, \qquad Ca = \frac{\mu U_s}{\gamma_0}, \qquad \alpha = \frac{\gamma_0 h}{\mu D_s}. \qquad (2.11)$$

Note that α is related to the surfactant surface Péclet number by $Pe = (L/h) Ca \alpha$. The definitions for Ca and α coincide with those of Ca' and α' employed by Pozrikidis (2003).

Considering the limit of long waves, we may extend the analysis of Benjamin (1957) and Yih (1963) to the case of a contaminated film, by expressing the perturbed streamfunction $\phi(y)$ and the complex wave speed c as a series expansion in integer powers of kh, as done by Whitaker & Jones (1966) and Lin (1970). These expansions are then substituted in the Orr–Sommerfeld equation (2.10) and accompanying boundary conditions (2.5)–(2.9) to yield a sequence of problems at each order of the reduced wavenumber. Following this procedure, we find

$$c = 2U_s + ikhU_s \left(\tfrac{8}{15} Re - \tfrac{2}{3} \cot \theta_0 - \frac{Ma}{Ca} \right) + \cdots, \qquad (2.12)$$

under the restrictive assumption $kh \ll 1$. Thus, long waves travel at twice the surface velocity of the unperturbed flow, and the flow is unstable for all Reynolds numbers greater than the critical value

$$\widehat{Re}_c = \tfrac{5}{4} \cot \theta_0 + \frac{15 Ma}{8 Ca}. \qquad (2.13)$$

In the absence of a surfactant, $Ma = 0$, we recover the classical results of Benjamin (1957) and Yih (1963), confirmed experimentally by Liu, Paul & Gollub (1993). According to (2.13), in the absence of surfactant, a vertical film corresponding to $\theta_0 = \pi/2$ is unstable at all Reynolds numbers. In contrast, when surfactant is present, the film is stable for sufficiently small Reynolds numbers. The same qualitative conclusion was reached by Benjamin (1964), who modelled the contaminated surface as a thin viscoelastic membrane assumed to be in equilibrium at any instant. Expression (2.13) gives a clear indication of the stabilizing influence of the surfactant under the uncertainty associated with the small-wavenumber expansion. In particular, the expansion appears to be capable of producing only one normal mode, and it is not clear that this mode is dominant. In what follows, we verify that (2.12) does indeed correspond to the mode with the largest growth rate by comparison with numerical solutions of the unsimplified Orr–Sommerfeld equation.

The Orr–Sommerfeld equation (2.10) accompanied by the boundary conditions (2.5)–(2.9) was solved numerically using a Chebyshev tau method (e.g. Orszag 1971; Dongarra, Straughan & Walker 1996). To implement the method, we map the film domain $0 \leqslant y \leqslant h$ onto the canonical interval $-1 \leqslant \hat{y} \leqslant 1$, writing $\hat{y} = (2y - h)/h$. Next, we expand the perturbed streamfunction in a truncated series of Chebyshev polynomials, $T_i(\hat{y})$, writing

$$\psi^{(1)}(\hat{y}) = \sum_{i=0}^{N} a_i T_i(\hat{y}), \tag{2.14}$$

where the a_i are unknown coefficients, and N is a specified truncation level. Substituting (2.14) in (2.10), and projecting the resulting equation onto $T_m(\hat{y})$, for $m = 0, \ldots N - 4$, under the Chebyshev inner product,

$$\langle T_m(\hat{y}), f(\hat{y}) \rangle = \int_{-1}^{1} \frac{1}{\sqrt{1 - \hat{y}^2}} T_m(\hat{y}) f(\hat{y}) \, \mathrm{d}\hat{y}, \tag{2.15}$$

we derive a system of $N - 3$ equations for the $N + 2$ coefficients a_i. All integrals involving Chebyshev polynomials and their derivatives in the projection may be computed exactly using known identities and recursive relations (e.g. Gottlieb & Orszag 1977, pp. 159–161). A further set of five equations are obtained by substituting (2.14) in the boundary conditions (2.5)–(2.9). The complete set of equations is ultimately compiled into the linear system

$$\boldsymbol{A} \cdot \boldsymbol{w} = \zeta \boldsymbol{B} \cdot \boldsymbol{w}, \tag{2.16}$$

where $\boldsymbol{w} = (a_0, \ldots, a_N, A_1)^T$, and $\boldsymbol{A}$, $\boldsymbol{B}$ are square matrices of size $N + 2$. The generalized eigenvalue problem (2.16) was solved using a NAG routine based on the QZ algorithm to obtain ζ, and hence the complex phase velocity, c, from which the dimensionless growth rate, $s = khc_i/U_s$, is extracted. To filter out spurious eigenmodes, the truncation level N is increased until genuine modes are clearly identified. Typically, $N = 25$ terms are sufficient to obtain a good level of accuracy at small and moderate Reynolds numbers. However, larger values of N are required to accurately resolve the eigenfunctions at high Reynolds numbers.

To test the reliability of the code, computations were carried out for Stokes flow, $Re = 0$, and the results were compared with the exact growth rates derived by Yih (1963) in the absence of surfactant, $Ma = 0$, given by

$$s = -\frac{\tau}{2\hat{k}} \frac{\sinh(2\hat{k}) - 2\hat{k}}{\cosh^2 \hat{k} + \hat{k}^2}, \tag{2.17}$$
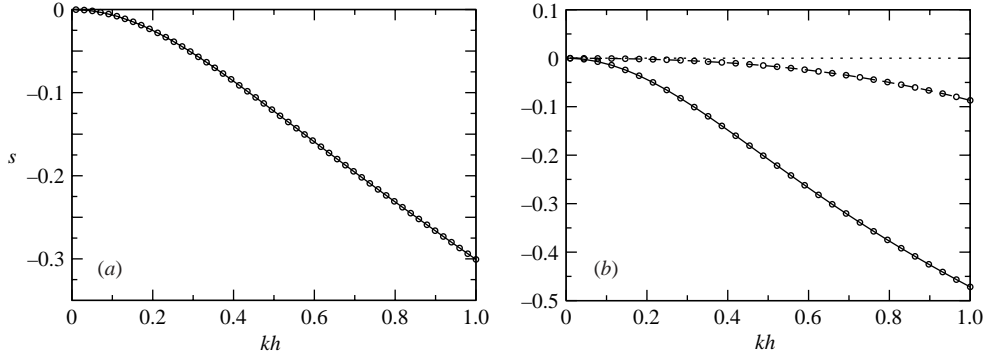
FIGURE 2. Growth rates for Stokes flow, $Re = 0$, for $Ca = 2.0$, $\theta_0 = \pi/4$. The lines correspond to the present results. (*a*) $Ma = 0$; the circles indicate the predictions of Yih (1963). (*b*) $Ma = 1.0$, $\alpha = 10.0$; the solid line corresponds to the Yih mode, the broken line to the Marangoni mode, and the circles indicate the predictions of Pozrikidis (2003).

where $\tau = \cot\theta_0 + \hat{k}^2/(2Ca)$ and $\hat{k} = kh$. Further comparisons were made with Pozrikidis's (2003) analytical predictions in the presence of surfactants, wherein the eigenvalues ζ satisfy a quadratic equation whose roots correspond to a pair of normal modes. Results obtained by the present numerical method for $Re = 0$ and $Ma = 0$ or $Ma = 1$ are in excellent agreement with the corresponding theoretical predictions, as shown figure 2.

The solid line in figure 2(*a*) represents the present results for $Ma = 0$, and the circles represent Yih's prediction (2.17). Because the growth rates are negative, the flow is stable for all reduced wavenumbers, kh. Results in the presence of surfactant shown in figure 2(*b*) reveal the occurrence of two normal modes, drawn with the solid and broken lines. The mode corresponding to the solid line is referred to as the Yih mode, and the mode corresponding to the broken line is referred to as the Marangoni mode. The growth rates computed by Pozrikidis (2003) by analytical methods are indicated by circles. Because the growth rates of both normal modes are negative, the flow is stable for any wavenumber. If the Marangoni number is continuously reduced to zero, the growth rate of the Yih mode collapses onto Yih's prediction (2.17) for a clean interface.

To test the reliability of the code for non-zero Reynolds numbers, the numerical results were compared with those reported by Chin, Abernathy & Bertschy (1986) for a clean film flow. Figure 3 shows the growth rate of the most dangerous mode, referred to as the gravity-mode by Chin *et al.*, for $Re = 2500$, $Ca = 0.017716$ and $\theta = 4°$. These conditions correspond to $\gamma_{cab} = 4280$, where γ_{cab} is Chin *et al.*'s dimensionless parameter, related to our parameters by $\gamma_{cab} = Re^{2/3}(\sin\theta_0)^{1/3}/Ca$. Our numerical results faithfully reproduce the growth rates presented by Chin *et al.* in their figure 5.

3. Results

The effect of inertia on the growth rates of the Yih and Marangoni modes is demonstrated in figure 4(*a*) for $Ca = 2.0$, $\alpha = 100$, $Ma = 1.0$, $\theta_0 = \pi/4$, and $kh = 0.5$. The growth rate for a clean interface is shown as a bold line originating from the Yih value given in (2.17) for $Re = 0$. The thin solid and broken lines represent, respectively, the growth rates for the Yih and Marangoni modes in the presence of surfactant, originating from values predicted by Pozrikidis (2003) for $Re = 0$. At small Reynolds numbers, the effect of the surfactant is twofold. First, the rate of decay of the Yih
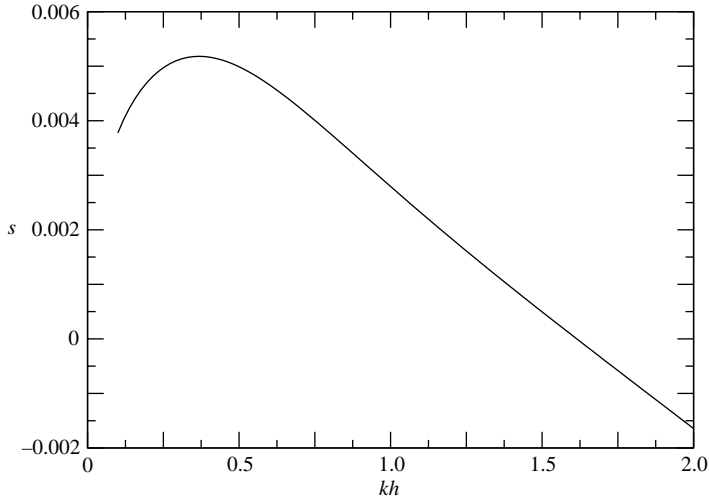
FIGURE 3. Dominant growth rate plotted against the reduced wavenumber for $Re = 2500$, $Ca = 0.017716$, $Ma = 0$, and $\theta_0 = 4°$.
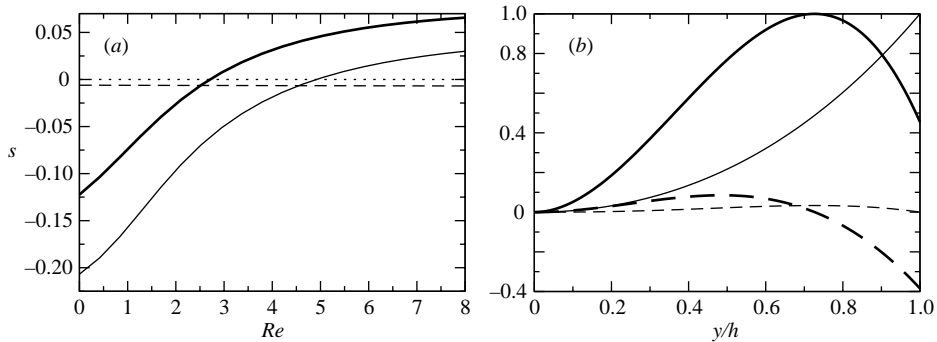

FIGURE 4. (*a*) Effect of inertia on the growth rates for a clean interface (bold line) and a contaminated interface with $Ma = 1$, for $Ca = 2.0$, $\alpha = 100$, $\theta_0 = \pi/4$, $kh = 0.5$. The thin solid line and broken line correspond to the Yih and Marangoni growth rates, respectively. (*b*) Eigenfunctions for $Ma = 1$ and $Re = 8.0$, with the real and imaginary parts shown as solid and broken lines respectively for the Yih mode (thin lines) and Marangoni mode (thick lines).

mode is increased, promoting the stability of the film flow. At the same time, a new normal mode is introduced with rate of decay significantly lower than that of the Yih mode prevailing at a clean interface. In this sense, the effect of the surfactant is destabilizing, though the film flow is in fact stable, as discussed by Pozrikidis (2003) and briefly summarized in §1.

Figure 4(*a*) shows that the Marangoni mode dominates only when the Reynolds number is sufficiently small. As the Reynolds number is raised, inertia causes an increase in the growth rate of the Yih mode until, ultimately, an exchange of stability occurs wherein the Yih mode claims the dominant role. During this exchange, the growth rate of the Marangoni mode hardly changes at all, and the corresponding perturbations remain stable. As the Reynolds number is further increased, the growth rate of the Yih mode eventually passes through zero, producing an unstable flow. With surfactant present, the onset of instability is delayed, as the thin solid line passes through zero well after the thick solid line. Thus, the primary role of the surfactant is to effectively raise the critical Reynolds number where instability first occurs, in
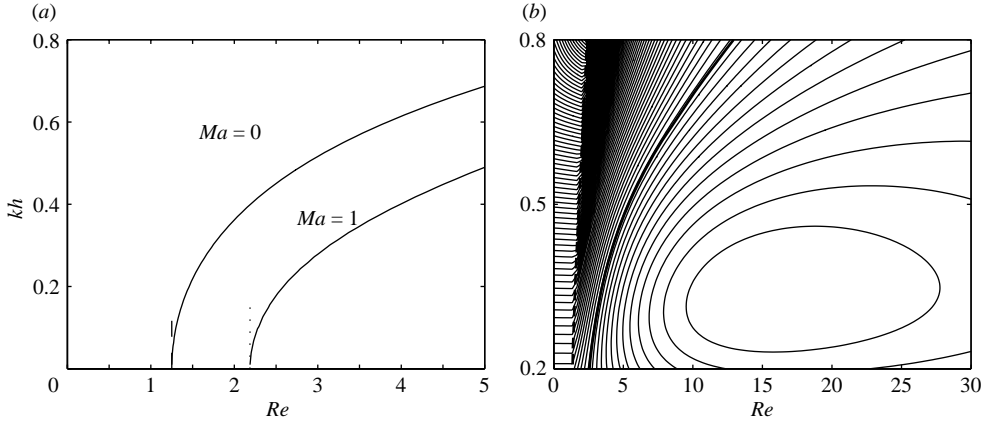
FIGURE 5. $Ca = 2.0$, $\alpha = 1$, $\theta_0 = \pi/4$: (a) Neutral stability curves for $Ma = 0$ and 1.0; the small-wavenumber critical Reynolds numbers $Re_c = 1.25$ and $\widehat{Re}_c = 2.1875$ are shown as broken and dotted lines respectively. (b) $Ma = 1.0$: Contours of the growth rate s, with the neutral curve shown as a heavy solid line and the mode-crossing shown as a heavy broken line.

agreement with the findings of previous authors. The eigenfunctions of the unstable Yih mode and the stable Marangoni mode at $Re = 8.0$ are shown in figure 4(b), normalized by their maximum moduli.

Neutral stability curves are shown in figure 5(a) for $Ca = 2.0$, $\alpha = 1.0$, $\theta_0 = \pi/4$, $Ma = 0$ or 1.0. The area to the left of each curve corresponds to stable modes, and the area to the right to unstable modes. When surfactant is introduced, the critical Reynolds number nearly doubles, and the neutral curve is shifted to the right. Also shown with broken lines in figure 5(a) are the predictions of the long-wave approximation expressed by (2.13); for a clean interface, $Re_c = 5/4$. In the limit $kh \to 0$, the numerical results are in excellent agreement with the theoretical predictions in the presence and absence of surfactants. It should be emphasized that the long-wave analysis does not preclude the possibility that the neutral curve doubles back on itself at larger wavenumbers, leading to a lower critical Reynolds number than that given by (2.13). However, we have not been able to find any examples where this occurs. Contours of the dimensionless growth rate s for $Ca = 2.0$, $\alpha = 1.0$, $\theta_0 = \pi/4$, and $Ma = 1.0$ are shown in figure 5(b), where the neutral curve is indicated by a bold solid line. The area underneath this curve corresponds to instability. Also shown as a bold broken line are the points where the mode-crossing highlighted in figure 4 occurs, for different parameters. The maximum growth rate, $s = 0.052$, occurs at $(Re, kh) = (15.44, 0.33)$.

The effect of the inclination angle, θ_0, on the neutral curve is illustrated in figure 6(a) for $Ca = 2.0$, $Ma = 1.0$ and $\alpha = 1.0$, where the region underneath each curve corresponds to instability. As the inclination angle is raised and the film tends to become vertical, the neutral curve is shifted upwards, widening the range of unstable wavenumbers at any given Reynolds number. The effect of the dimensionless parameter α is shown in figure 6(b) for $Ca = 2.0$, $Ma = 1.0$ and $\theta = \pi/4$. Increasing α amounts to decreasing surfactant diffusivity. The results show that the stability characteristics of the film are insensitive to the surfactant diffusivity up to about $Re \sim 10$. Beyond this threshold, marked differences are observed in the neutral curves for different values of α.

We have seen that, at sufficiently large Reynolds numbers, the Yih mode dominates and is responsible for flow instability. However, additional 'shear' modes associated with the underlying half-plane Poiseuille base flow are also present (Chin *et al.* 1986).
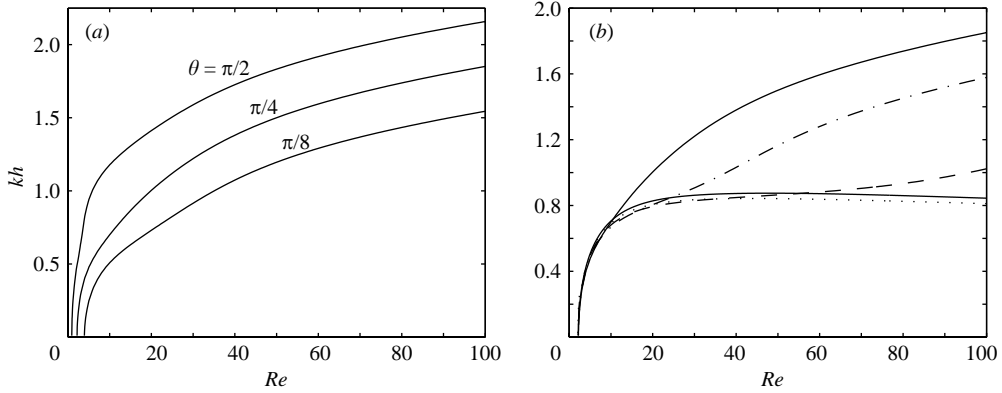
FIGURE 6. Neutral stability curves for $Ca = 2.0$, $Ma = 1.0$: (a) $\alpha = 1.0$ and for the three inclination angles $\theta = \pi/2$, $\pi/4$, $\pi/8$. (b) $\theta = \pi/4$ and $\alpha = 1.0$ (upper solid line), $\alpha = 2.5$ (dashed-dotted line), $\alpha = 5.0$ (dashed line), $\alpha = 10.0$ (dotted line) and $\alpha = 100.0$ (lower solid line).
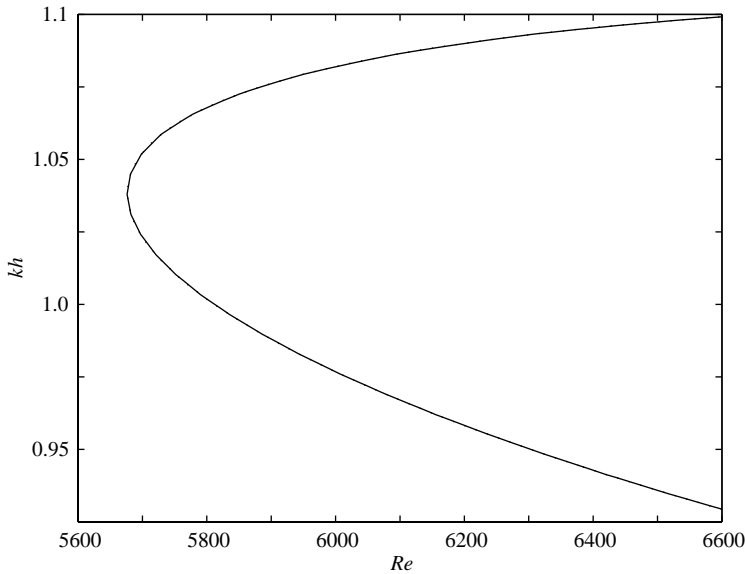

FIGURE 7. Neutral stability curves for $\gamma_{cab} = 4280$, and $\theta = 4°$. The two curves for $Ma = 0$ and 1 are indistinguishable.

The critical Reynolds number associated with the most unstable shear mode is approximately $Re_c = 5676$, which is close to that for plane Poiseuille flow, $Re_c = 5772.2$ (e.g. Orzsag 1971). In figure 7, we present the neutral curve for the most unstable shear mode, together with the corresponding curve for a contaminated surface with $Ma = 1.0$. The results reveal that the surfactant has little effect on the shear modes, which are described well by the channel-flow solution.

4. Discussion

We have solved the linear stability problem for a liquid film flowing down an inclined plane at arbitrary Reynolds numbers, and quantified the simultaneous effect of

inertia and Marangoni tractions due to an insoluble surfactant. The numerical method was validated by successful comparison with previous results available in the literature.

We have shown that the effect of an insoluble surfactant is predominantly benign, as it tends to calm the film surface. At zero Reynolds number, two normal modes arise. The first, the Yih mode, is associated with the disturbance wave superimposed on the film surface, and the second, the Marangoni mode, is associated with the periodic spatial variation in the surfactant concentration. The rate of decay of the Marangoni mode is significantly lower than that for the Yih mode. However, as the Reynolds number is increased from zero, the growth rate of the Yih mode increases, while that for the Marangoni mode remains virtually constant. Eventually, while both growth rates are still negative, the Yih mode overtakes the Marangoni mode, before becoming unstable.

In the absence of surfactant, only the Yih mode is present. Its growth rate rises with increasing inertia, producing instability at a critical value of the Reynolds number. When surfactant is introduced onto the film's surface, this critical Reynolds number increases. Thus, overall, the surfactant has a stabilizing effect on the film dynamics.

REFERENCES

ANSHUS, B. E. & ACRIVOS, A. 1967 The effect of surface-active agents on the stability characteristics of falling liquid films. *Chem. Engng Sci.* **22**, 389–393.

BENJAMIN, T. B. 1957 Wave formation in laminar flow down an inclined plane. *J. Fluid Mech.* **2**, 554–574.

BENJAMIN, T. B. 1964 Effect of surface contamination on wave formation in falling liquid films. *Archwm. Mech. Stosow.* **16**, 615–626.

CHIN, R. W., ABERNATHY, F. H. & BERTSCHY, J. R. 1986 Gravity and shear wave stability of free surface flows. Part 1. Numerical calculations. *J. Fluid Mech.* **168**, 501–513.

DONGARRA, J. J., STRAUGHAN, B. & WALKER, D. W. 1996 Chebyshev tau-QZ algorithm methods for calculating spectra of hydrodynamic stability problems. *Appl. Numer. Maths* **22**, 399–434.

GOTTLIEB, D. & ORSZAG, S. A. 1977 *Numerical Analysis of Spectral Methods*. SIAM.

JI, W. & SETTERWALL, F. 1994 On the instabilities of vertical falling liquid films in the presence of surface-active solute. *J. Fluid Mech.* **278**, 297–323.

LI, X. F. & POZRIKIDIS, C. 1997 The effect of surfactants on drop deformation and on the rheology of dilute emulsions in Stokes flow. *J. Fluid Mech.* **341**, 165–194.

LIN, S. P. 1970 Stabilizing effects of surface-active agents on a film flow. *AIChE* **16**, 375–379.

LIU, J., PAUL, J. D. & GOLLUB, J. P. 1993 Measurements of the primary instabilities of film flows. *J. Fluid Mech.* **250**, 69–101.

ORSZAG, S. A. 1971 Accurate solution of the Orr-Sommerfeld stability equation. *J. Fluid Mech.* **50**, 689–703.

POZRIKIDIS, C. 1997 *Introduction to Theoretical and Computational Fluid Dynamics*. Oxford University Press.

POZRIKIDIS, C. 2003 Effect of surfactants on film flow down a periodic wall. *J. Fluid Mech.* **496**, 105–127.

WEINSTEIN, S. J. & RUSCHAK, K. J. 2004 Coating flows. *Annu. Rev. Fluid Mech.* **36**, 29–53.

WHITAKER, S. 1964 Effect of surface active agents on the stability of falling liquid films. *Ind. Engng Chem. Fundam* **3**, 132–142.

WHITAKER, S. & JONES, L. O. 1966 Stability of falling liquid films. Effect of interface and interfacial mass transport. *AIChE J.* **12**, 421–431.

YIH, C. S. 1963 Stability of a liquid flow down an inclined plane. *Phys. Fluids* **6**, 321–334.

YON, S. & POZRIKIDIS, C. 1998 A finite-volume/boundary-element method for flow past interfaces in the presence of surfactants, with application to shear flow past a viscous drop. *Computers Fluids* **27**, 879–902.